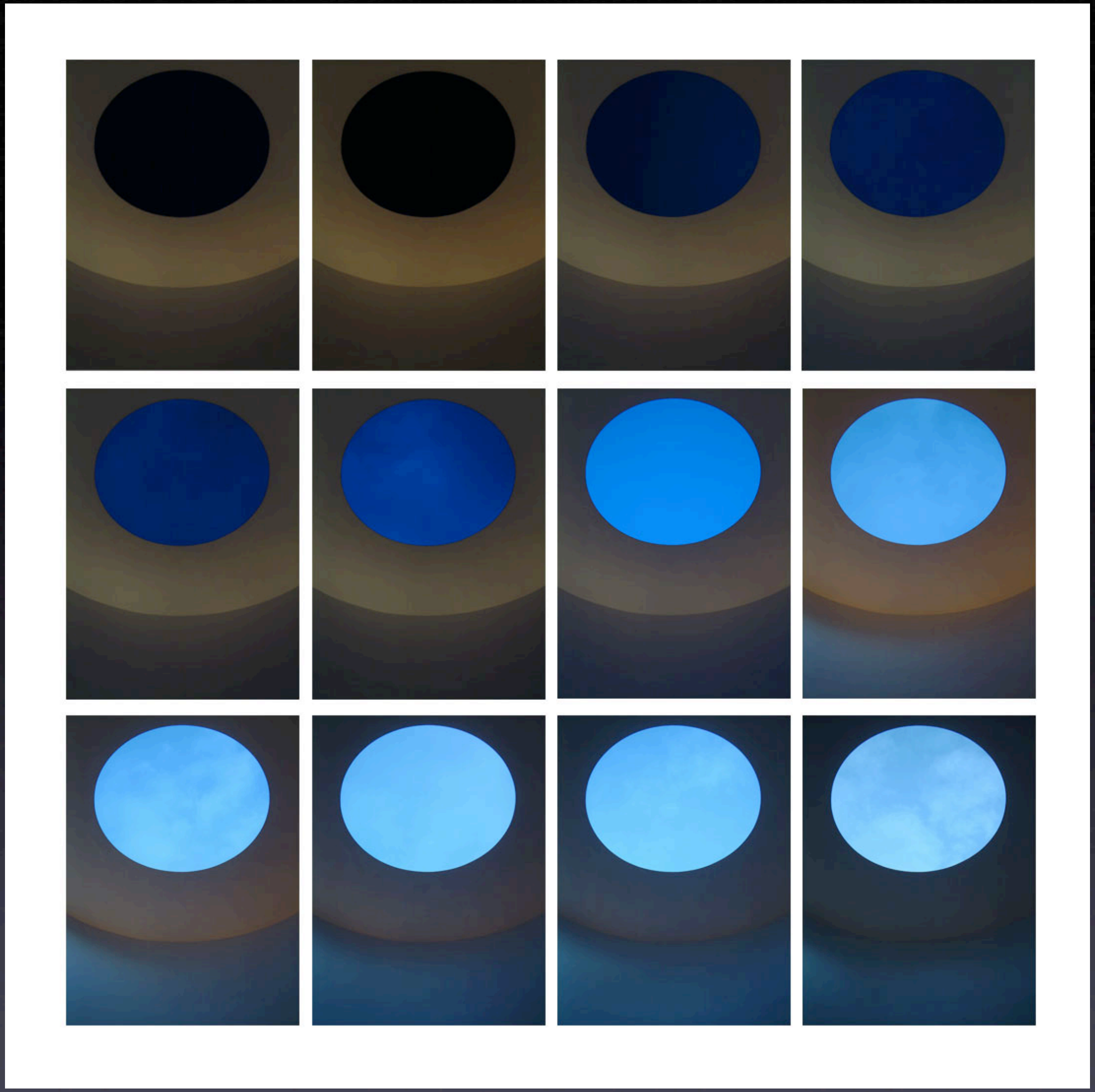

evolution and global properties of hot jupiters

gregory laughlin - uco/lick observatory

Collaborators

- Mark Ammons, Peter Bodenheimer, Paul Butler, Debra Fischer, Greg Henry Shigeru Ida, Geoff Marcy, Sally Robinson, Jay Strader, Bunei Sato, Steve Vogt, Aaron Wolf
- Funding from the NASA TPF Program and the NSF CAREER Program

HD 149026b

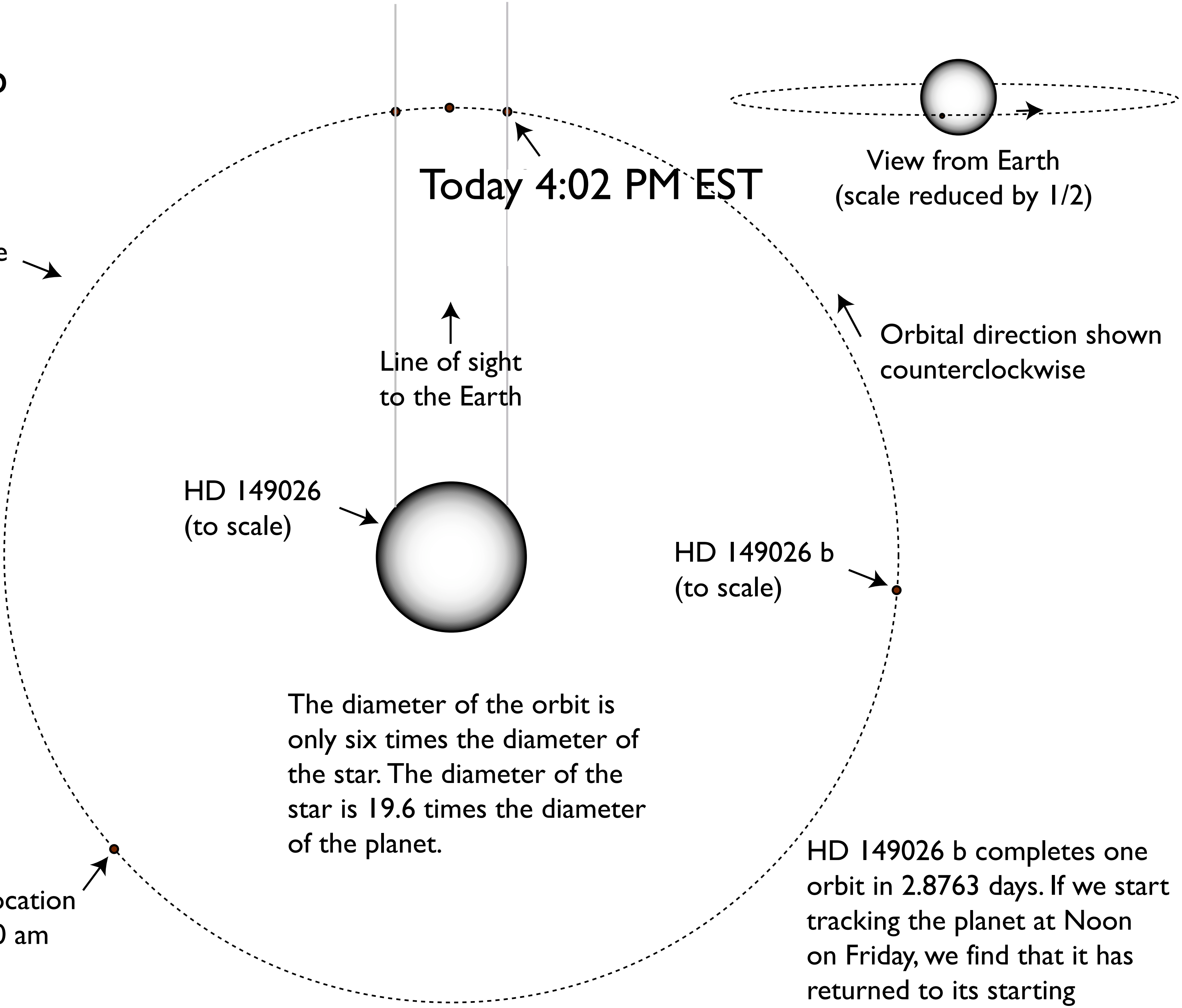

Today 4:02 PM EST

View from Earth
(scale reduced by 1/2)

Viewed from above

Line of sight
to the Earth

Orbital direction shown
counterclockwise

Orbital path
(to scale)

HD 149026
(to scale)

HD 149026 b
(to scale)

The diameter of the orbit is only six times the diameter of the star. The diameter of the star is 19.6 times the diameter of the planet.

Planet location
Sun. 5:00 am

HD 149026 b completes one orbit in 2.8763 days. If we start tracking the planet at Noon on Friday, we find that it has returned to its starting position by 9:01 am on Monday morning.

The Known Transiting Planets

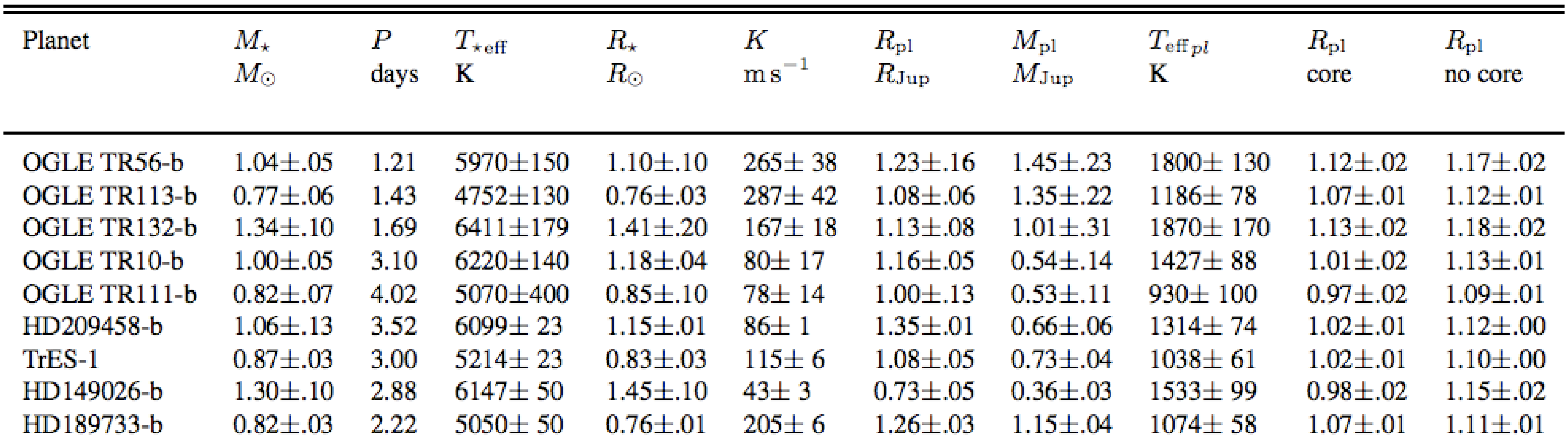

Planet	$M_\star$ $M_\odot$	P days	$T_{\star\mathrm{eff}}$ K	$R_\star$ $R_\odot$	K $\mathrm{m\,s^{-1}}$	R_{pl} R_{Jup}	M_{pl} M_{Jup}	$T_{\mathrm{eff}\,pl}$ K	R_{pl} core	R_{pl} no core
OGLE TR56-b	1.04±.05	1.21	5970±150	1.10±.10	265± 38	1.23±.16	1.45±.23	1800± 130	1.12±.02	1.17±.02
OGLE TR113-b	0.77±.06	1.43	4752±130	0.76±.03	287± 42	1.08±.06	1.35±.22	1186± 78	1.07±.01	1.12±.01
OGLE TR132-b	1.34±.10	1.69	6411±179	1.41±.20	167± 18	1.13±.08	1.01±.31	1870± 170	1.13±.02	1.18±.02
OGLE TR10-b	1.00±.05	3.10	6220±140	1.18±.04	80± 17	1.16±.05	0.54±.14	1427± 88	1.01±.02	1.13±.01
OGLE TR111-b	0.82±.07	4.02	5070±400	0.85±.10	78± 14	1.00±.13	0.53±.11	930± 100	0.97±.02	1.09±.01
HD209458-b	1.06±.13	3.52	6099± 23	1.15±.01	86± 1	1.35±.01	0.66±.06	1314± 74	1.02±.01	1.12±.00
TrES-1	0.87±.03	3.00	5214± 23	0.83±.03	115± 6	1.08±.05	0.73±.04	1038± 61	1.02±.01	1.10±.00
HD149026-b	1.30±.10	2.88	6147± 50	1.45±.10	43± 3	0.73±.05	0.36±.03	1533± 99	0.98±.02	1.15±.02
HD189733-b	0.82±.03	2.22	5050± 50	0.76±.01	205± 6	1.26±.03	1.15±.04	1074± 58	1.07±.01	1.11±.01

Model Predictions

HD 209458b and HD 189733b “too large”
HD 149026b “too small”

Radius determination for HD 149026
(Wolf et al 2006)

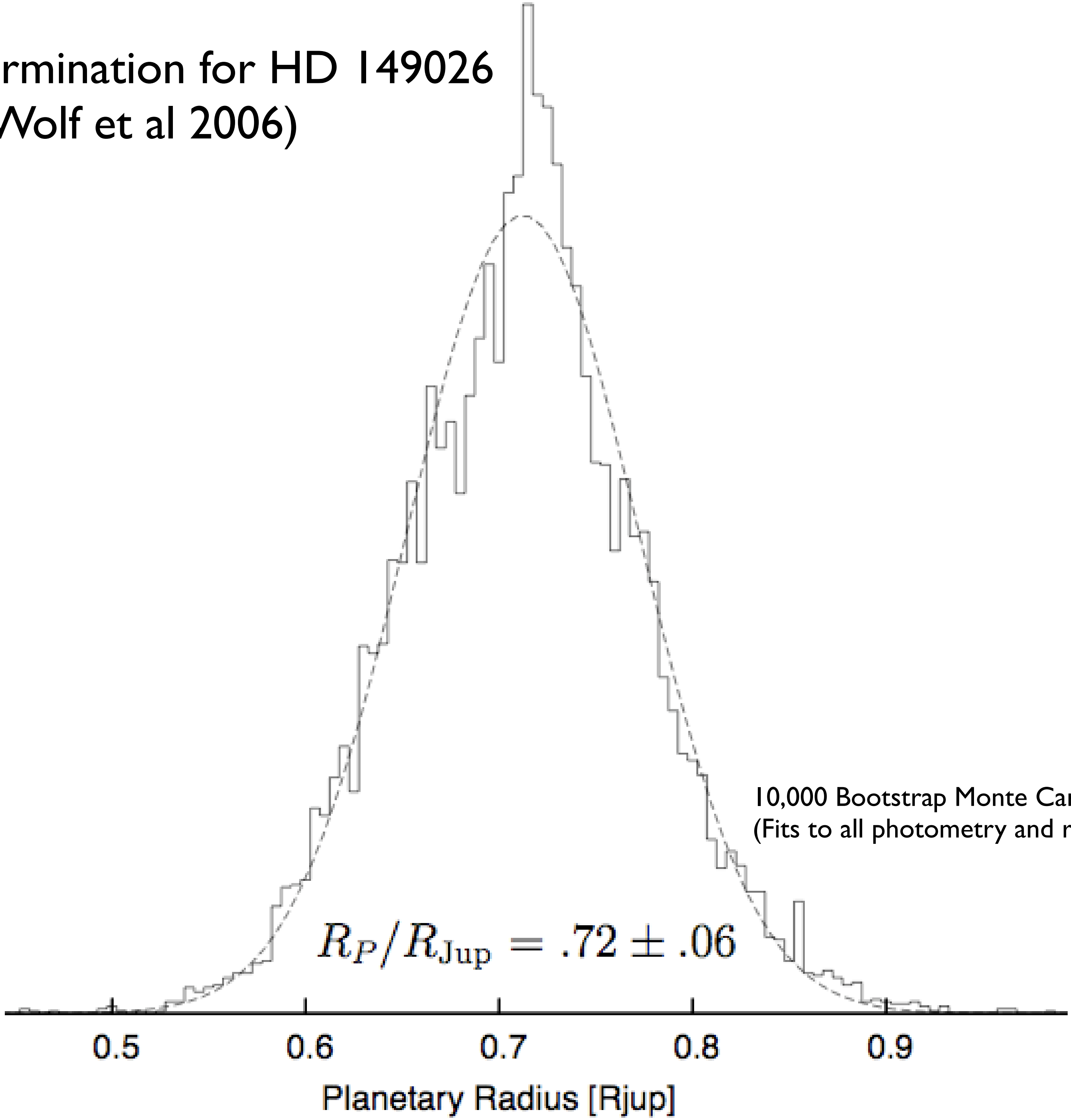

$$R_P/R_{\rm Jup} = .72 \pm .06$$

10,000 Bootstrap Monte Carlo Trials
(Fits to all photometry and radial velocities)

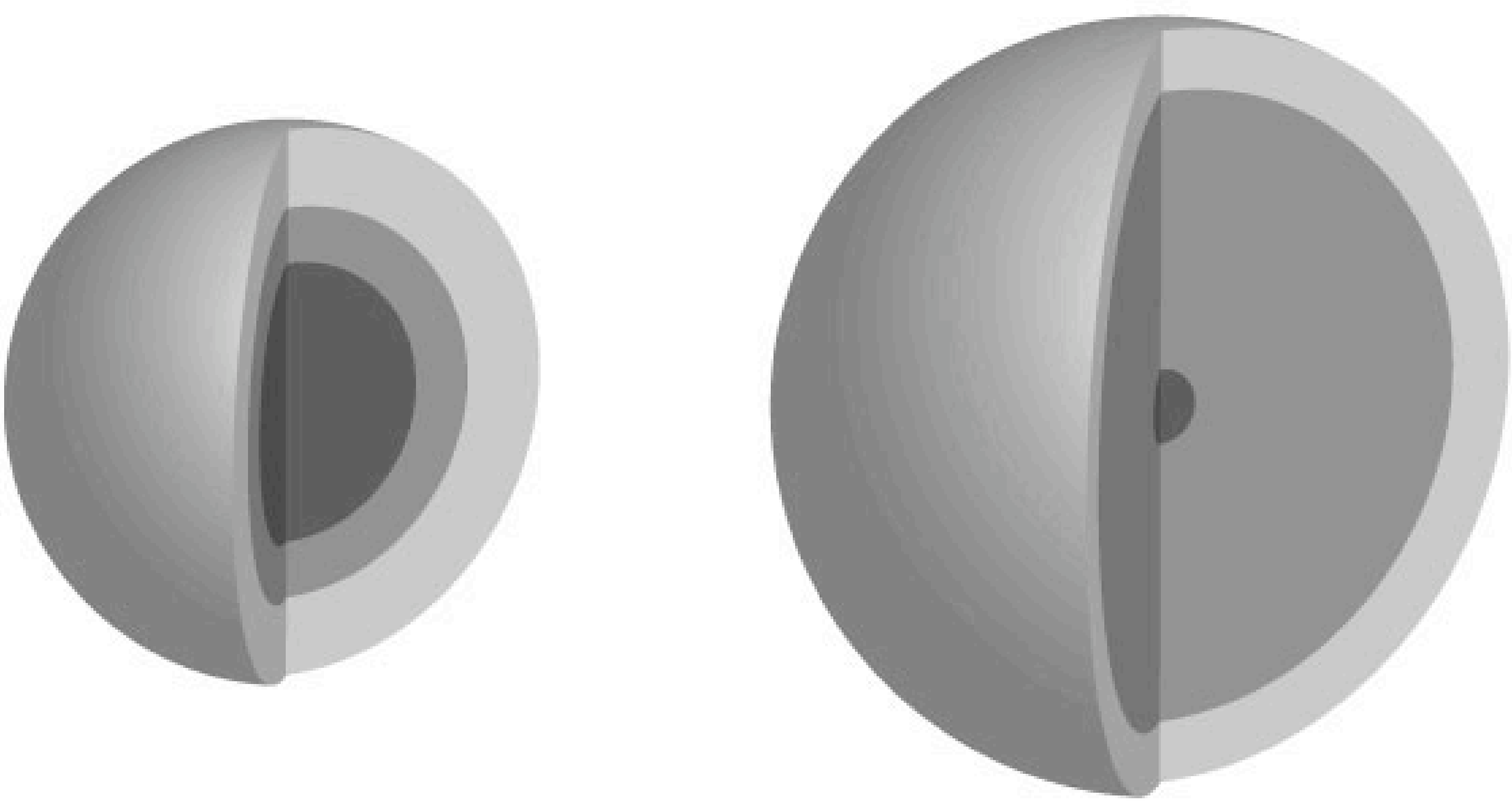

R/Rjup	R/Rjup	Mcore
10.5 gm/cc	5.5 gm/cc	
0.594	0.662	89.3
0.681	0.745	74.5
0.769	0.818	60.0
0.866	0.905	43.6

▢	molecular hydrogen and helium
▨	liquid metallic hydrogen
■	heavy element core

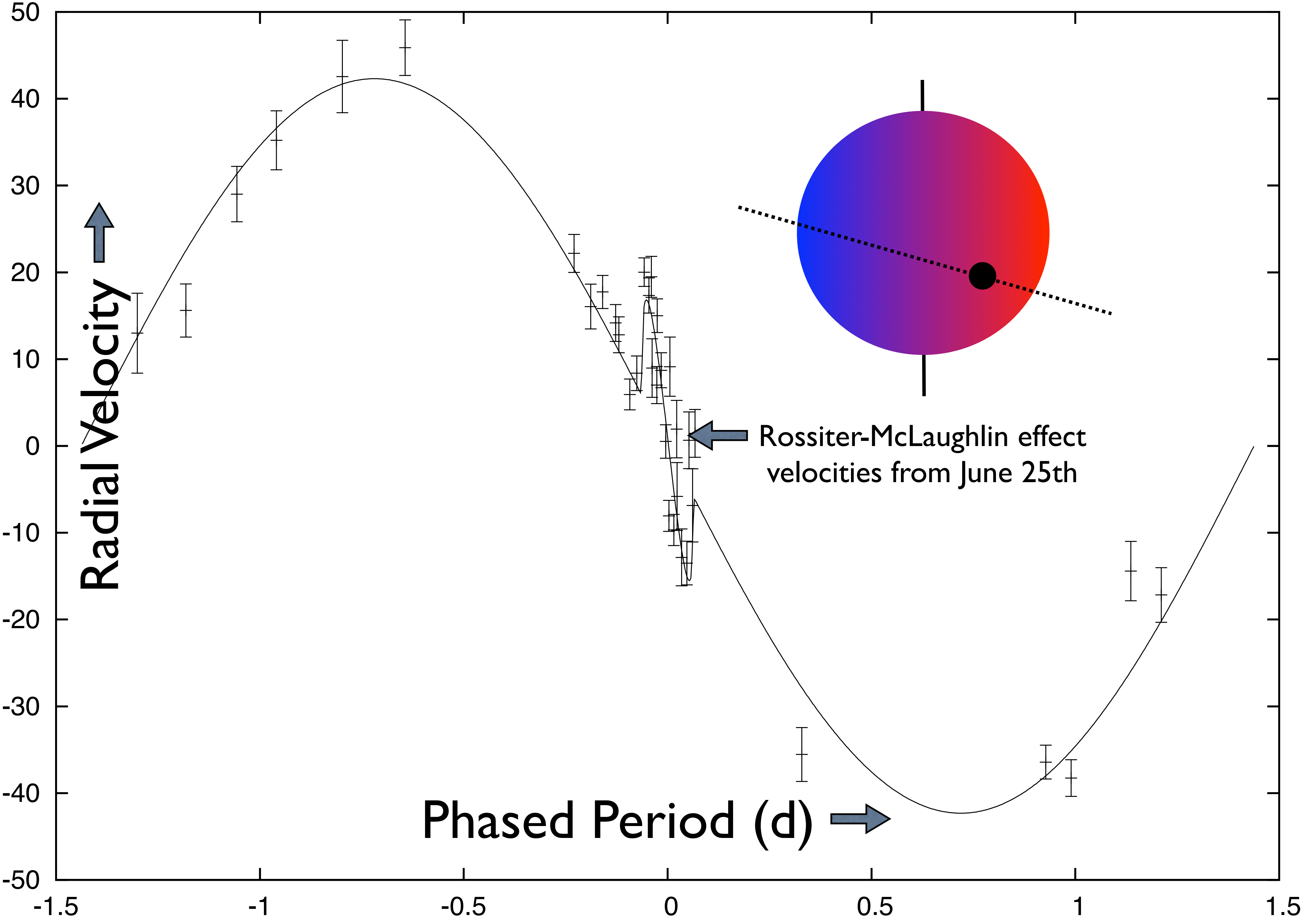

Rossiter-McLaughlin effect velocities from June 25th

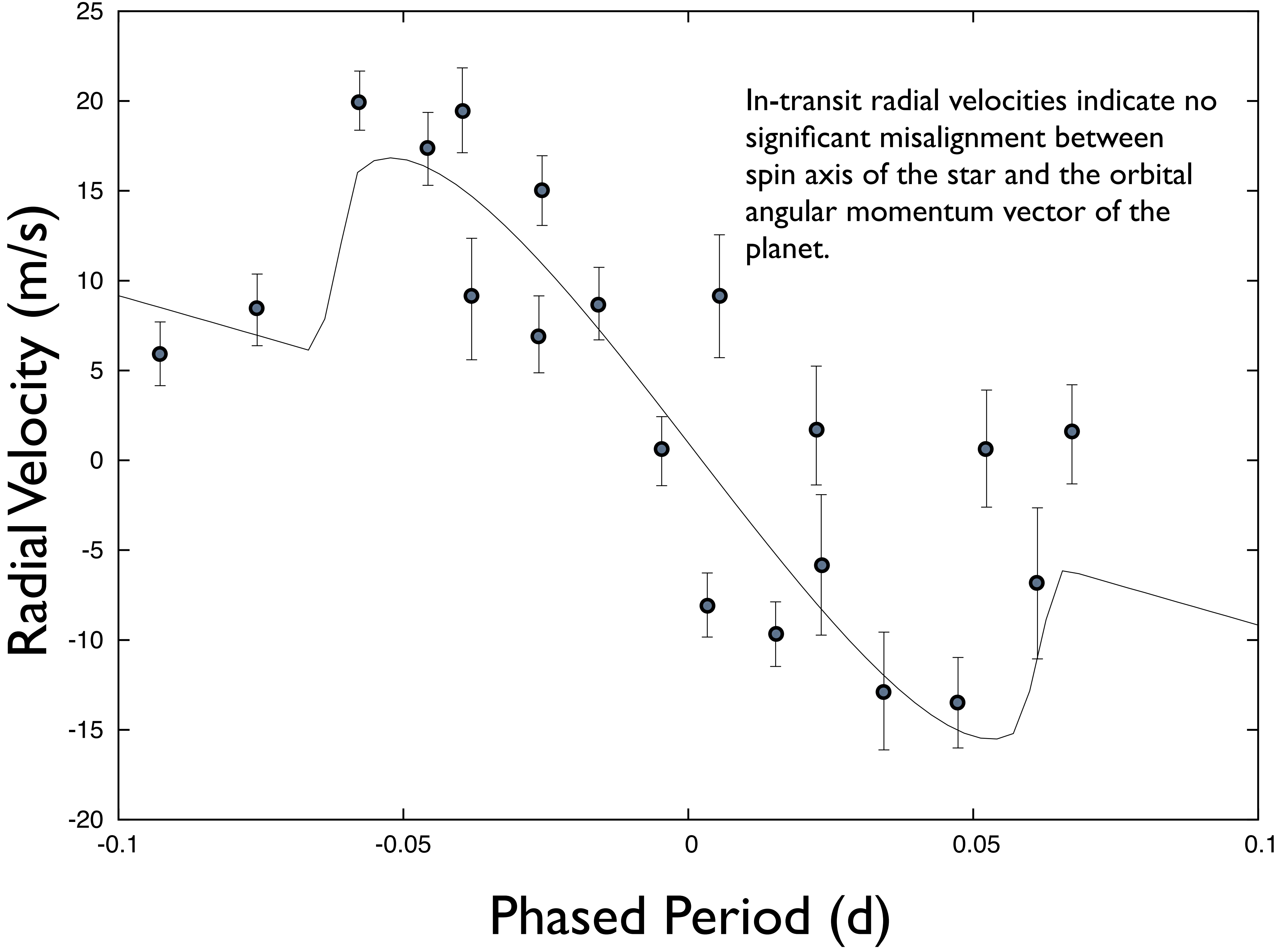

In-transit radial velocities indicate no significant misalignment between spin axis of the star and the orbital angular momentum vector of the planet.

10,000 bootstrap trials

(Wolf et al. 2006)

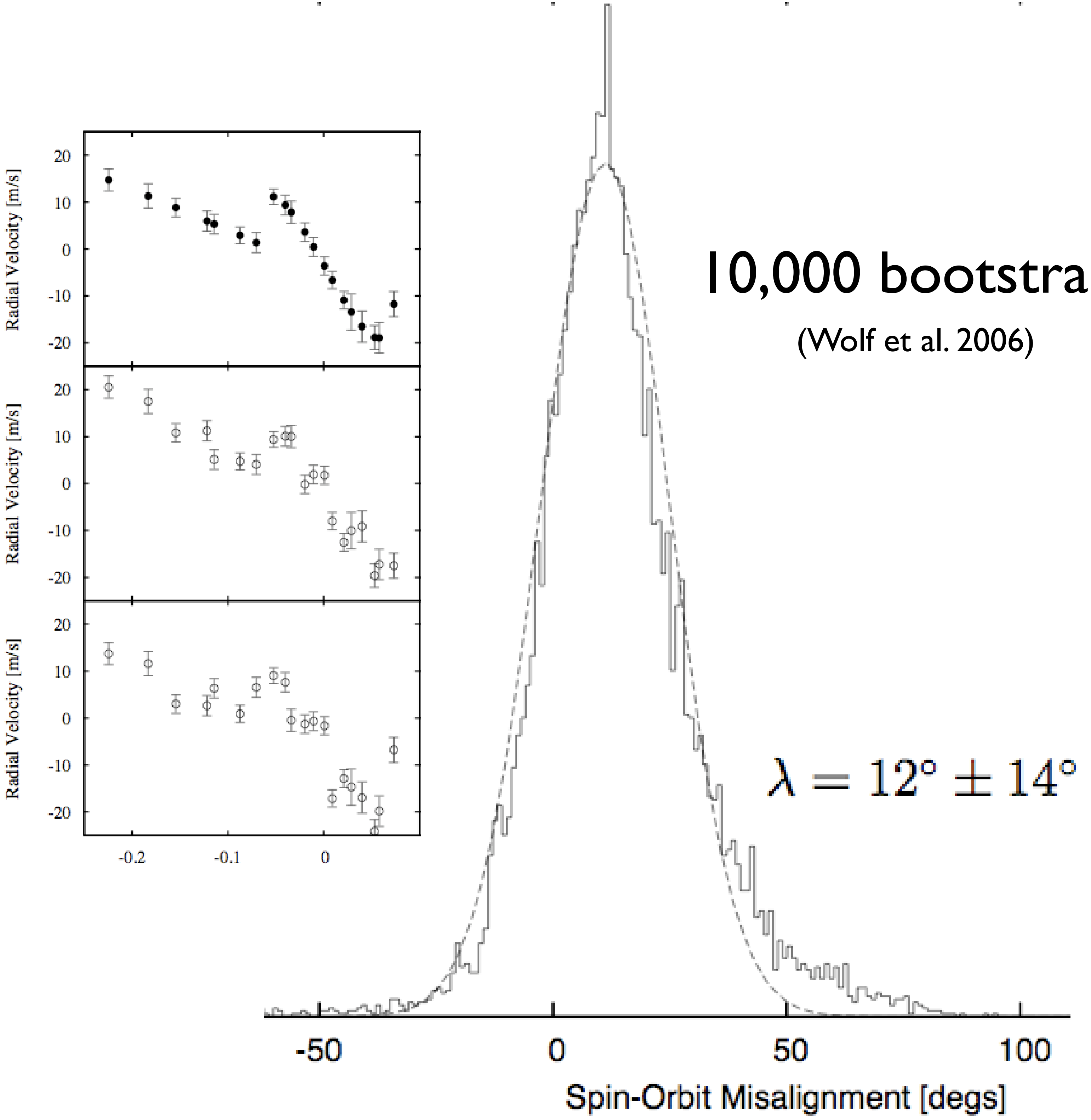

$\lambda = 12° \pm 14°$

The Known Transiting Planets

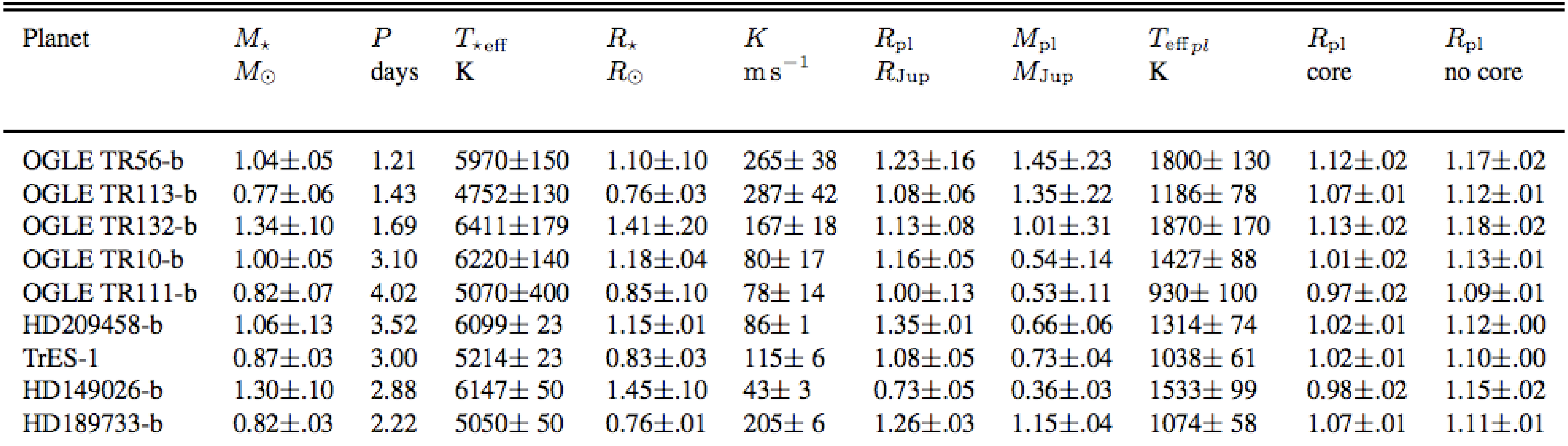

Planet	$M_\star$ $M_\odot$	P days	$T_{\star \mathrm{eff}}$ K	$R_\star$ $R_\odot$	K $\mathrm{m\,s^{-1}}$	R_{pl} R_{Jup}	M_{pl} M_{Jup}	$T_{\mathrm{eff}\,pl}$ K	R_{pl} core	R_{pl} no core
OGLE TR56-b	1.04±.05	1.21	5970±150	1.10±.10	265± 38	1.23±.16	1.45±.23	1800± 130	1.12±.02	1.17±.02
OGLE TR113-b	0.77±.06	1.43	4752±130	0.76±.03	287± 42	1.08±.06	1.35±.22	1186± 78	1.07±.01	1.12±.01
OGLE TR132-b	1.34±.10	1.69	6411±179	1.41±.20	167± 18	1.13±.08	1.01±.31	1870± 170	1.13±.02	1.18±.02
OGLE TR10-b	1.00±.05	3.10	6220±140	1.18±.04	80± 17	1.16±.05	0.54±.14	1427± 88	1.01±.02	1.13±.01
OGLE TR111-b	0.82±.07	4.02	5070±400	0.85±.10	78± 14	1.00±.13	0.53±.11	930± 100	0.97±.02	1.09±.01
HD209458-b	1.06±.13	3.52	6099± 23	1.15±.01	86± 1	1.35±.01	0.66±.06	1314± 74	1.02±.01	1.12±.00
TrES-1	0.87±.03	3.00	5214± 23	0.83±.03	115± 6	1.08±.05	0.73±.04	1038± 61	1.02±.01	1.10±.00
HD149026-b	1.30±.10	2.88	6147± 50	1.45±.10	43± 3	0.73±.05	0.36±.03	1533± 99	0.98±.02	1.15±.02
HD189733-b	0.82±.03	2.22	5050± 50	0.76±.01	205± 6	1.26±.03	1.15±.04	1074± 58	1.07±.01	1.11±.01

Model Predictions

HD 209458b and HD 189733b “too large”

HD 149026b “too small”

IRTF view of Jupiter in Near-IR

The Core Accretion Paradigm

Perri & Cameron 1974, Mizuno et al 1978, Mizuno 1980, Bodenheimer & Pollack 1986, Pollack et al 1996

During Phase 1, the growing planet consists mostly of solid material. The planet experiences runaway accretion until the feeding zone is depleted. Solid accretion occurs much faster than gas accretion during this phase.

During Phase 2, both solid and gas accretion rates are small and are nearly independent of time. This phase dictates the overall evolutionary time-scale.

During Phase 3, runaway gas accretion occurs. Runaway gas accretion starts when the solid and gas masses are roughly equal.

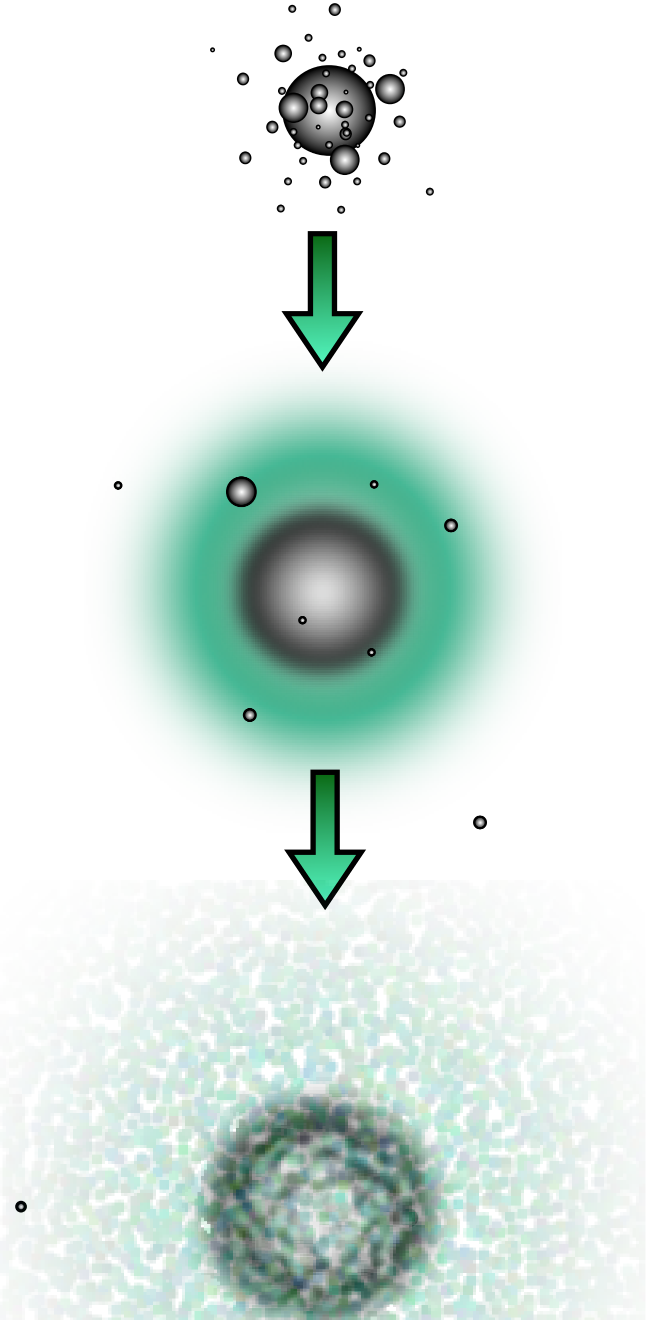

A key (and well established) result of standard core accretion theory is the extraordinary sensitivity of the time of onset of rapid gas accretion to the surface density of solids in the disk.

Recent calculations by Hubickyj et al (2005), illustrate that decreasing the solid surface density from 10 to 6 gm/cm2 causes a 12 Myr delay in the onset of rapid gas accretion. This solid surface density decrease corresponds to a ~0.2 dex decrease in metallicity.

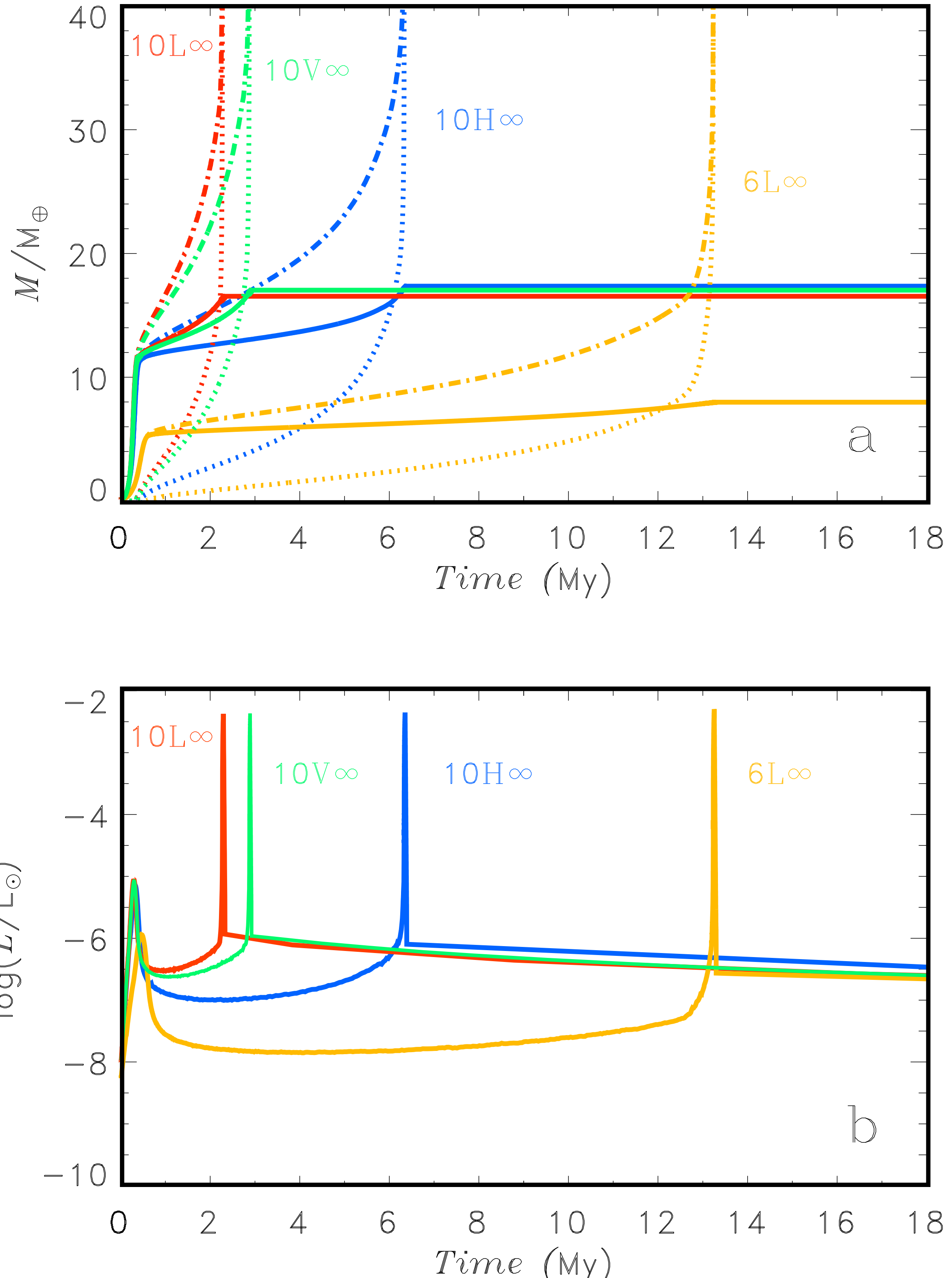

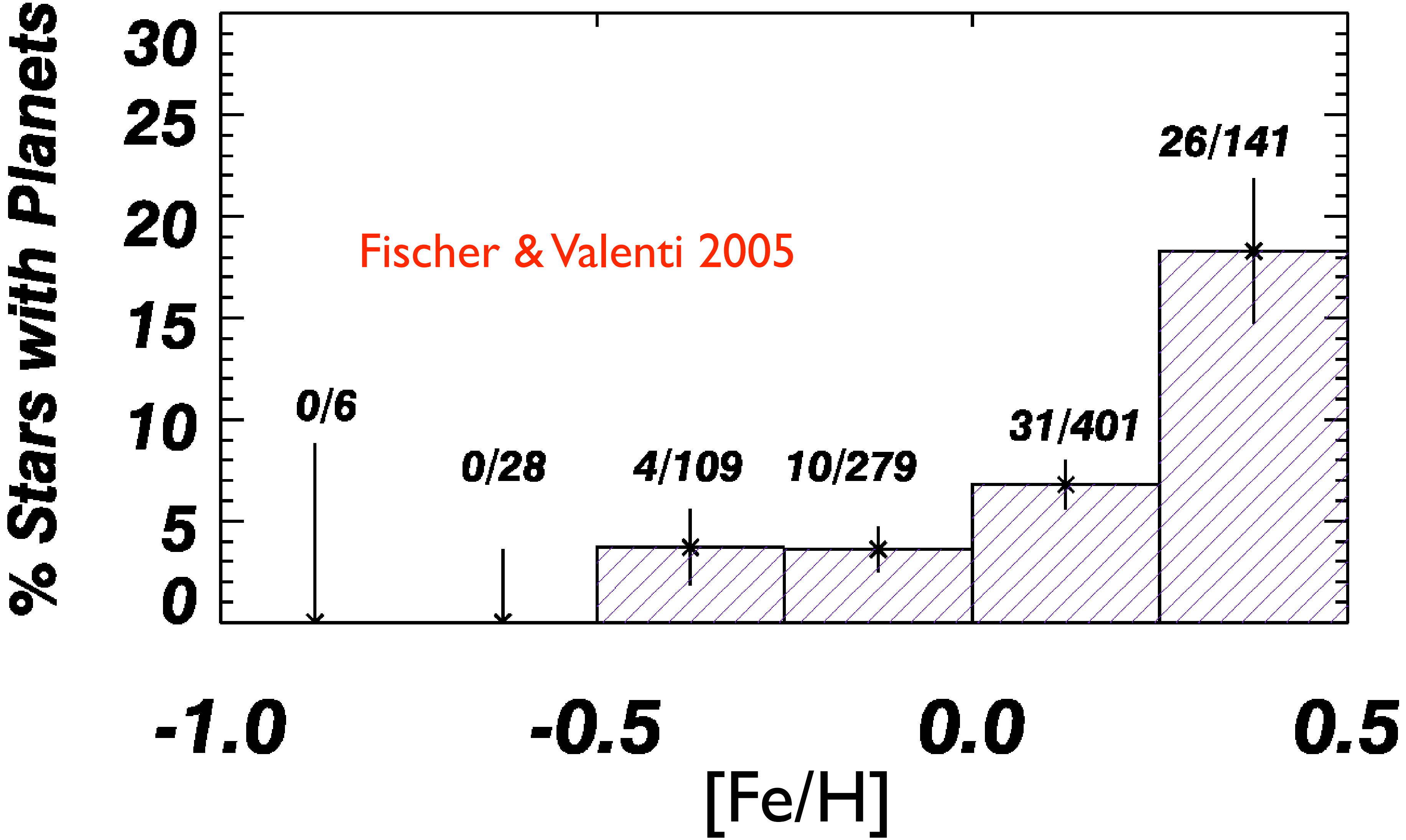

The extrasolar planet - host star metallicity connection is one of the most remarkable results to have emerged from the radial velocity surveys. The correlation can be interpreted as being the outcome of the sensitive dependance of core accretion on the surface density of solids in the protostellar disks.

Tests of the Core Accretion Theory

The sensitive dependance of the core accretion timescale on surface density is independant of the other controlling parameters. If this effect is responsible for the observed metallicity correlation, one expects that Jovian-mass planet formation should also proceed more easily in higher mass disks. If disk-to-star mass ratios are relatively constant, then there should also be a stellar mass correlation with planet frequency.

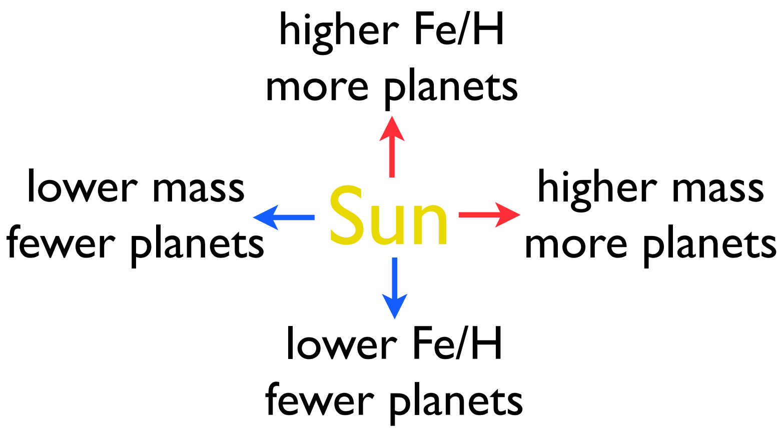

higher Fe/H
more planets

lower mass
fewer planets

Sun

higher mass
more planets

lower Fe/H
fewer planets

Another test of the Core Accretion Theory

The sensitive dependance of the core accretion timescale on surface density is independant of the other controlling parameters. If this effect is responsible for the observed metallicity correlation, one also expects that at given Fe/H, the planet frequency should increase with O/Fe, and to a slightly lesser extent with Si/Fe (Si and O are both core forming elements, and they are produced primarily in Type II supernovae, and hence have correlated abundances.

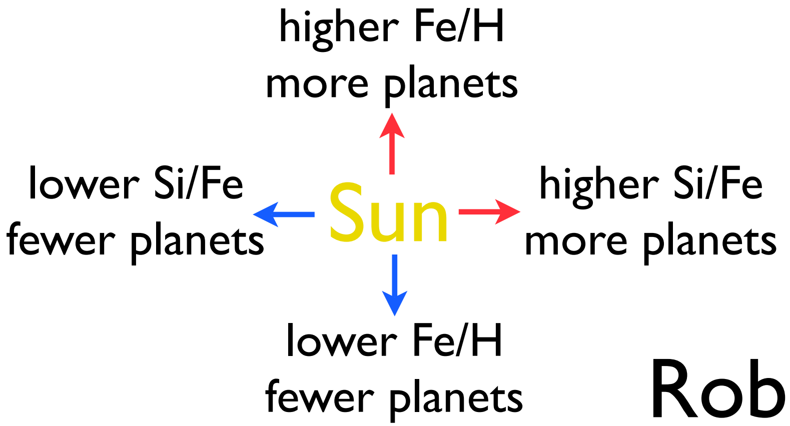

higher Fe/H
more planets

lower Si/Fe
fewer planets

Sun

higher Si/Fe
more planets

lower Fe/H
fewer planets

Robinson et al. 2006

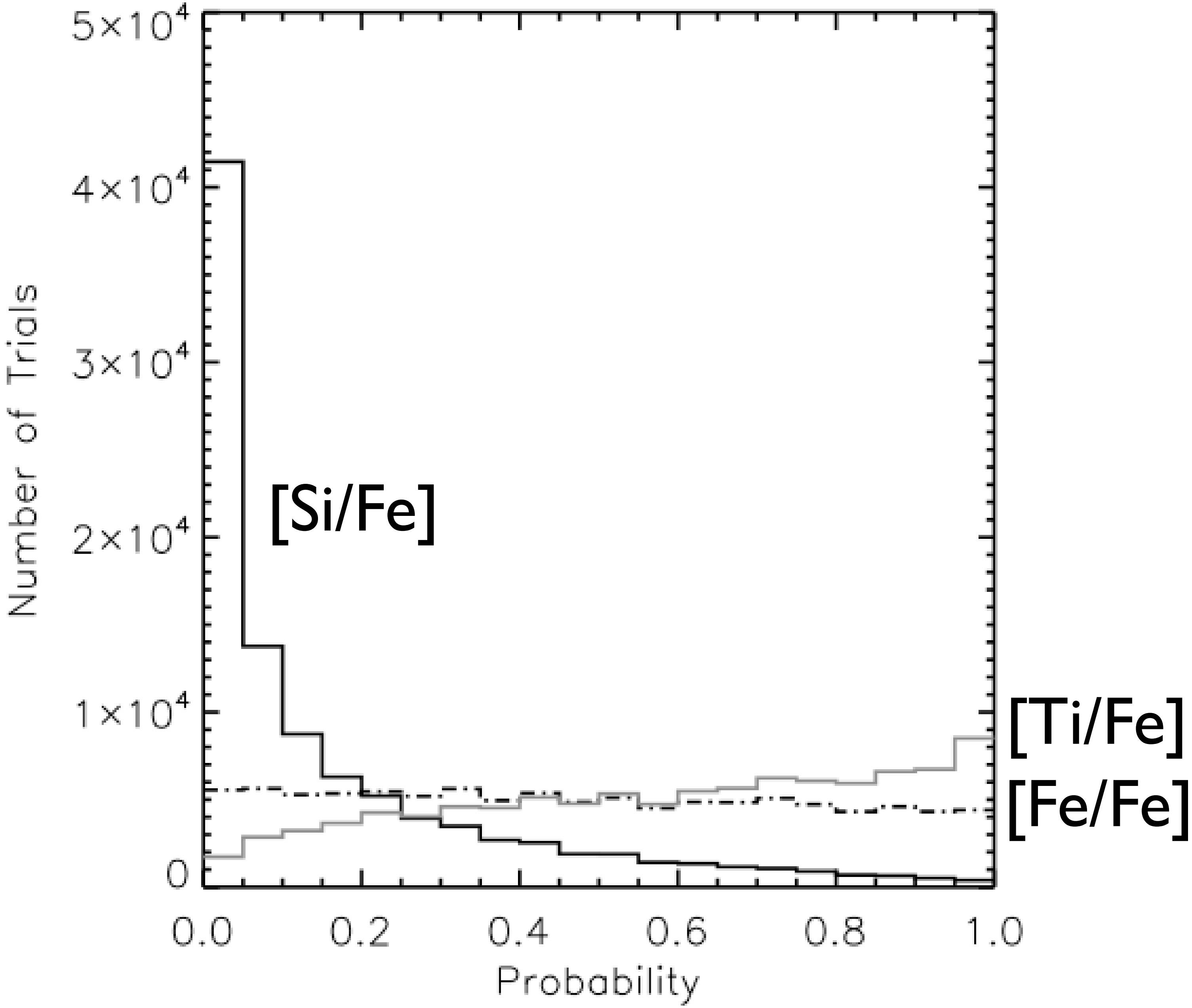

Robinson et al. (2006) show that stars with an enhanced Si/Fe ratio at given Fe have a higher probability of harboring a detectable planet

Predictions

Core-accretion based Planet formation model described in Robinson et al.(2006) predicts that the Silicon effect should be slightly less evident than suggested by the current observational data set.

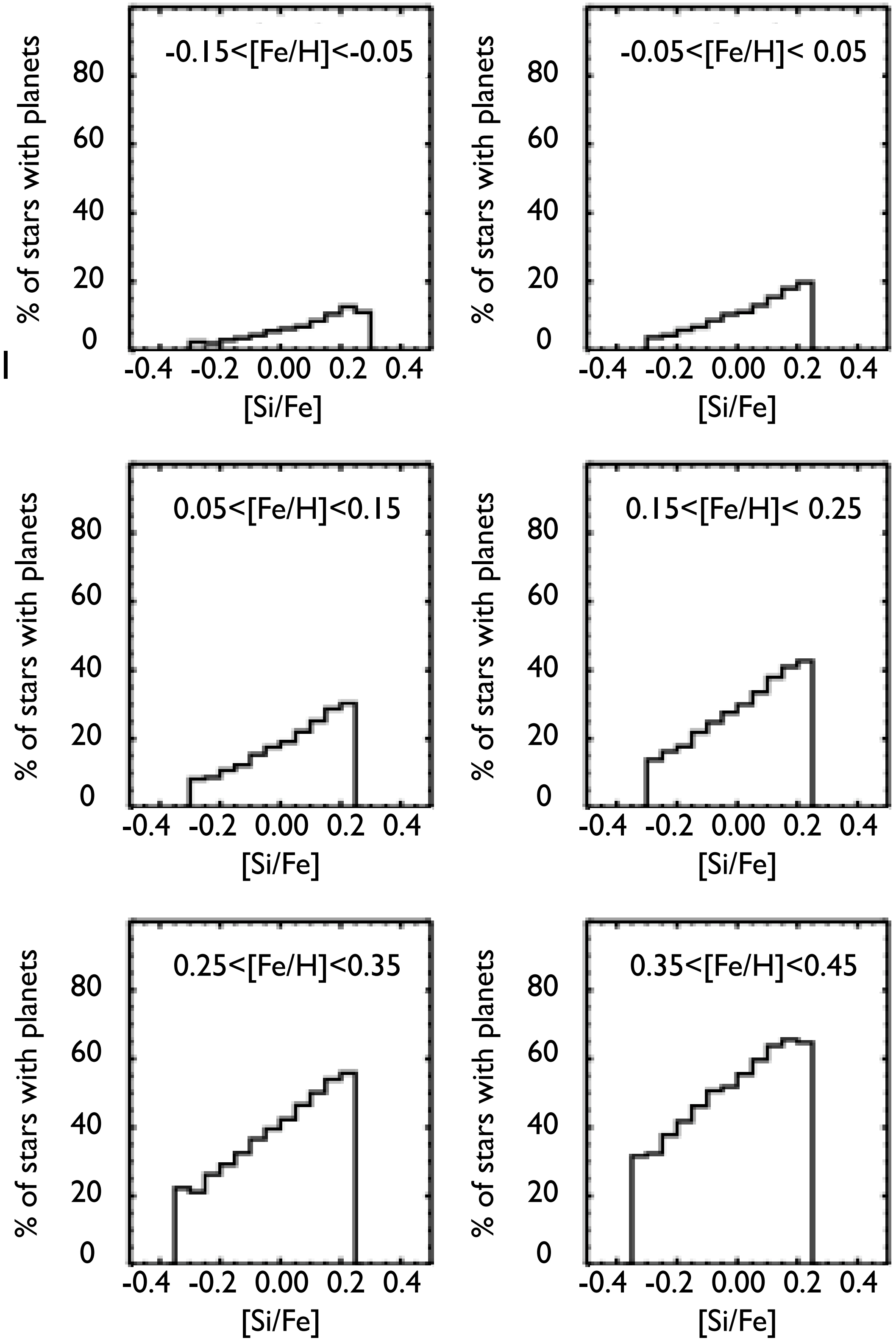

www.oklo.org

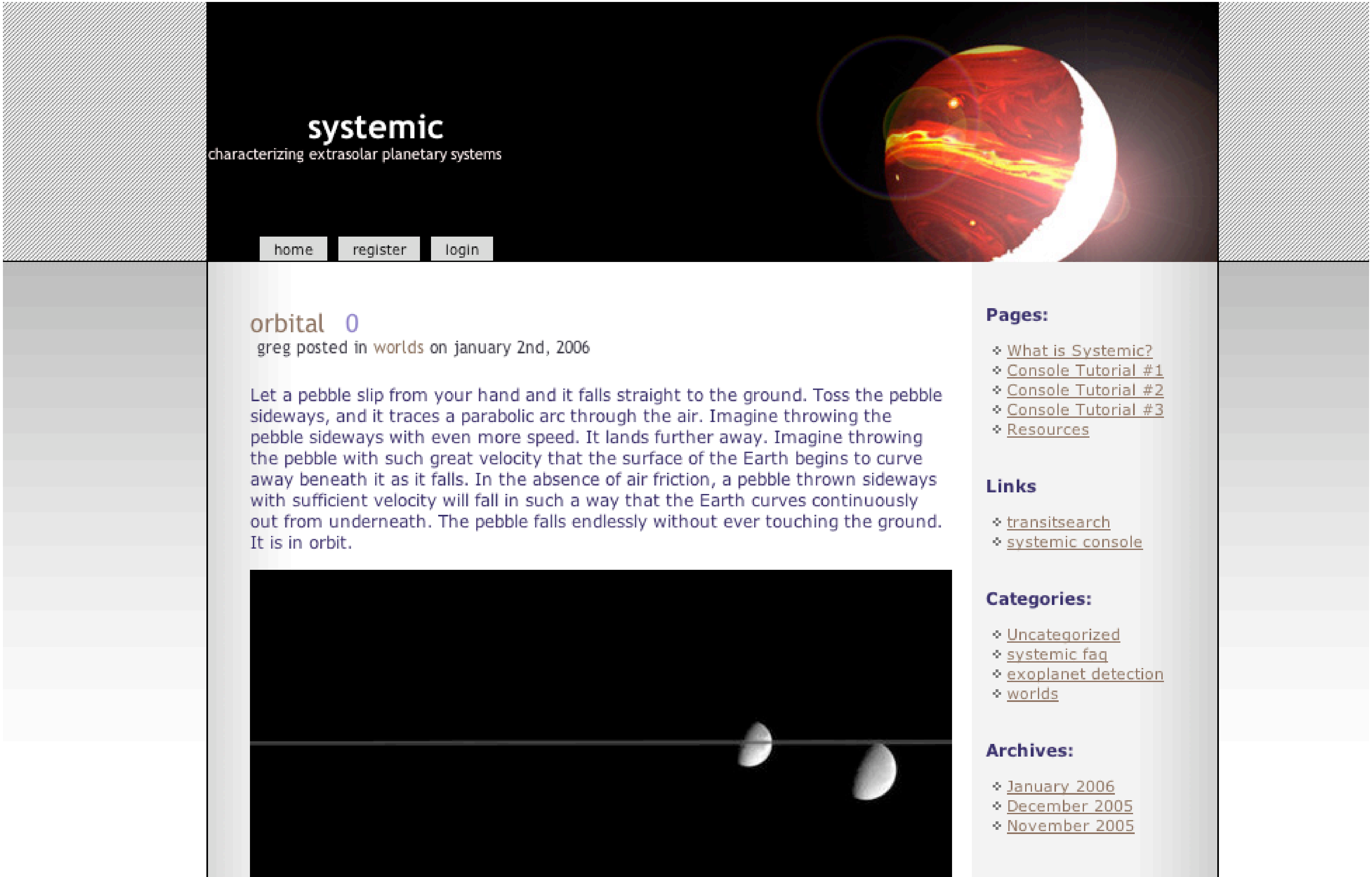

orbital 0

greg posted in worlds on january 2nd, 2006

Let a pebble slip from your hand and it falls straight to the ground. Toss the pebble sideways, and it traces a parabolic arc through the air. Imagine throwing the pebble sideways with even more speed. It lands further away. Imagine throwing the pebble with such great velocity that the surface of the Earth begins to curve away beneath it as it falls. In the absence of air friction, a pebble thrown sideways with sufficient velocity will fall in such a way that the Earth curves continuously out from underneath. The pebble falls endlessly without ever touching the ground. It is in orbit.

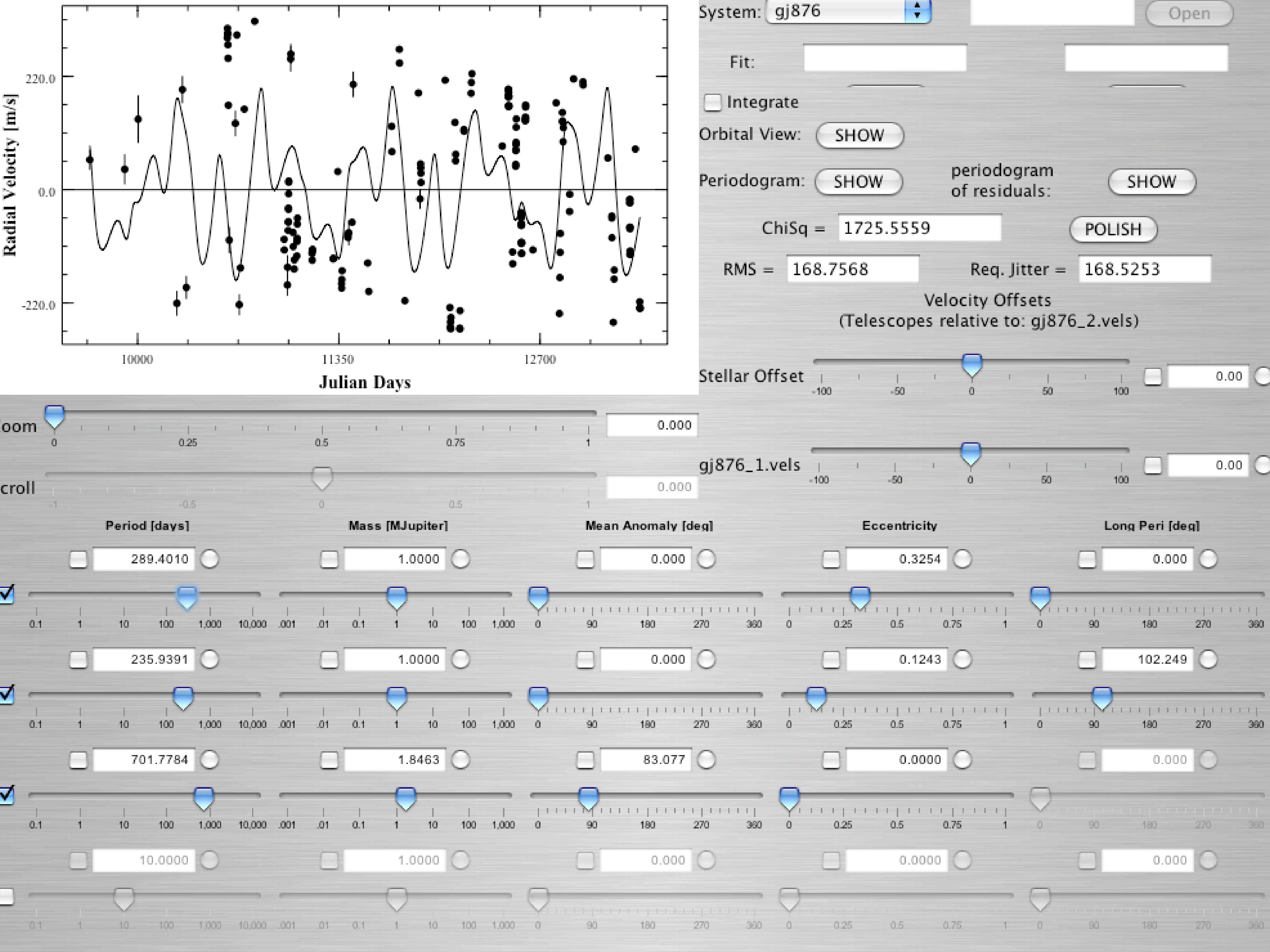

System: gj876

Fit:

☐ Integrate

Orbital View: SHOW

Periodogram: SHOW

periodogram of residuals: SHOW

ChiSq = 1725.5559

RMS = 168.7568

Req. Jitter = 168.5253

Velocity Offsets
(Telescopes relative to: gj876_2.vels)

Stellar Offset ☐ 0.00

gj876_1.vels ☐ 0.00

oom 0.000

croll 0.000

	Period [days]	Mass [MJupiter]	Mean Anomaly [deg]	Eccentricity	Long Peri [deg]
☑	289.4010	1.0000	0.000	0.3254	0.000
☑	235.9391	1.0000	0.000	0.1243	102.249
☑	701.7784	1.8463	83.077	0.0000	0.000
☐	10.0000	1.0000	0.000	0.0000	0.000

www.oklo.org